

# Nitroxyl Radicals for Labeling of Conventional Therapeutics and Noninvasive Magnetic Resonance Imaging of Their Permeability for Blood–Brain Barrier: Relationship between Structure, Blood Clearance, and MRI Signal Dynamic in the Brain

Zhivko Zhelev,<sup>†</sup> Rumiana Bakalova,<sup>\*,†</sup> Ichio Aoki,<sup>†</sup> Ken-ichiro Matsumoto,<sup>‡</sup>  
Veselina Gadjeva,<sup>§</sup> Kazunori Anzai,<sup>‡</sup> and Iwao Kanno<sup>†</sup>

Department of Biophysics, Molecular Imaging Center, and Center for Heavy-ion Particle Therapy, National Institute of Radiological Sciences, 4-9-1 Anagawa, Inage-ku, Chiba 263-8555, Japan, and Department of Chemistry and Biochemistry, Trakia University, Stara Zagora, Bulgaria

Received September 24, 2008; Revised Manuscript Received January 7, 2009; Accepted January 9, 2009

**Abstract:** The present study describes a novel nonradioactive methodology for *in vivo* noninvasive, real-time imaging of blood–brain barrier (BBB) permeability for conventional drugs, using nitroxyl radicals as spin-labels and magnetic resonance imaging (MRI). Two TEMPO-labeled analogues (SLENU and SLCNUgly) of the anticancer drug lomustine [1-(2-chloroethyl)-3-cyclohexyl-1-nitrosourea] were synthesized, using a substitution of the cyclohexyl part with nitroxyl radical. Nonmodified nitroxyl radical TEMPOL was used for comparison. The nitroxyl derivatives were injected intravenously in healthy mice via the tail vein, and MR imaging of the brain was performed on a 7.0 T MRI. The MRI signal dynamic of SLENU and SLCNUgly followed the same kinetics as nonmodified TEMPO radical. SLENU and SLCNUgly were rapidly transported and randomly distributed in the brain tissue, which indicated that the exchange of cyclohexyl part of lomustine with TEMPO radical did not suppress the permeability of the anticancer drug for BBB. The selected nitroxyl derivatives possessed different hydrophobicity, cell permeabilization ability, and blood clearance. Based on these differences, we investigated the relationship between the structure of nitroxyl derivatives, their half-life in the circulation, and their MRI signal dynamic in the brain. This information was important for estimation of the merits and demerits of the described methodology and finding pathways for overcoming the restrictions.

**Keywords:** Nitroxyl radicals; lomustine; magnetic resonance imaging; electron-paramagnetic resonance imaging; blood–brain barrier permeability

## Introduction

The nitroxyl radicals are well-known from electron-paramagnetic resonance (EPR) studies.<sup>1–6</sup> In 1984, it was

reported that nitroxyl radicals possess comparatively high  $T_1$  contrast properties and could be also applied in magnetic resonance imaging (MRI).<sup>2,7</sup> The nitroxyls are small molecules, sensitive to the reduction status of biological samples, and their use in life science research is limited predominantly to tissue oxygen and redox mapping *in vitro* and *in vivo*.<sup>3–6,8–13</sup> The paramagnetic nitroxyl radical could be reduced to diamagnetic hydroxylamine with a loss of EPR signal or <sup>1</sup>H-MRI relaxation time and thus serve as a reduction sensor. However, the diamagnetic hydroxylamine

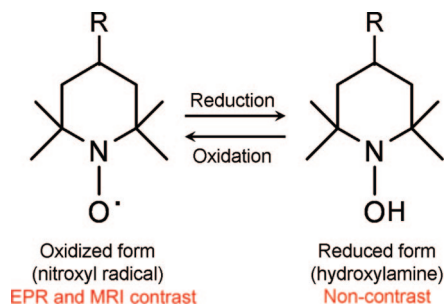
\* Author to whom correspondence should be addressed. Rumiana Bakalova, PhD, Department of Biophysics, Molecular Imaging Center, National Institute of Radiological Sciences (NIRS), 4-9-1 Anagawa, Inage-ku, Chiba 263-8555, Japan. Tel: +81-43-206-4067. Fax: +81-43-206-3276. E-mail: bakalova@nirs.go.jp; ra\_bakalova@yahoo.com.

<sup>†</sup> Department of Biophysics, Molecular Imaging Center, National Institute of Radiological Sciences.

<sup>‡</sup> Center for Heavy-ion Particle Therapy, National Institute of Radiological Sciences.

<sup>§</sup> Trakia University.

(1) Griffeth, L. K.; Rosen, G. M.; Rauckman, E. J.; Drayer, B. P. Pharmacokinetics of nitroxide NMR contrast agents. *Invest. Radiol.* **1984**, *19*, 553–562.

**Scheme 1.** Nitroxyl Radical Reduction and Oxidation Sensors

could be reconverted via oxygenation to paramagnetic nitroxyl radical with an appearance of EPR or  $^1\text{H}$ -MRI relaxivity and thus serve as an oxidation sensor. The rate constants of both processes could be used for evaluation of reduction/oxidation balance in cells and tissues, using EPR imaging (EPRI) or MRI (Scheme 1).

Some nitroxyl radicals can easily gain an excellent cell permeability and even a permeability for blood–brain barrier (BBB) by simple chemical modification.<sup>11–15</sup> All these characteristics make them attractive for MRI diagnostics, and their application in life science research could be extended beyond the limits, mentioned above. In this context, we supposed that the nitroxyl radicals could be appropriate spin-labels of conventional therapeutics: for noninvasive MR imaging of their permeability for BBB and their localization in different organs and tissues. Most EPR studies, targeting the brain, have employed pyrrolidine-type (PROXYL-type) nitroxyl radicals, which have a higher stability *in vivo* in comparison with piperidine-type (TEMPO-type) nitroxyl radicals due to the low temporal resolution of CW-based techniques.<sup>12–15</sup> The higher temporal resolution of MRI allows an observation of pharmacokinetics of piperidine-type nitroxyl radicals.<sup>9,16</sup> In addition, MRI is characterized by much higher spatial resolution than EPRI and gives an excellent anatomical reference, which could facilitate the

exact localization of a nitroxyl-labeled drug in the organism. Below, we would like to describe the impact of this approach and to give a proof for the reality of this concept.

The noninvasive, real-time imaging of drug permeability for BBB and localization in different brain compartments (drug brain mapping) is an indispensable step in the pre-clinical and clinical testing of new therapeutics for brain diseases. The precise mapping of a drug in the target or nontarget tissue has a significant impact for its dosing and prognostication of its target-specific effect and side effects.

The conventional methods for investigation of BBB permeability are usually invasive and time- and cost-consuming, often suffering from artifacts, and requiring a large number of experimental animals.<sup>17–22</sup> *In vitro* models of BBB (e.g., cell and tissue cultures, immobilized artificial

- (2) Keana, J. F.; Pou, S.; Rosen, G. M. Nitroxides as potential contrast enhancing agents for MRI application: influence of structure on the rate of reduction by rat hepatocytes, whole liver homogenate, subcellular fractions, and ascorbate. *Magn. Reson. Med.* **1987**, *5*, 525–536.
- (3) Valgimigli, L.; Pedulli, G. F.; Paolini, M. Measurement of oxidative stress by EPR radical-probe technique. *Free Radical Biol. Med.* **2001**, *31*, 708–716.
- (4) Utsumi, H.; Yamada, K. In vivo electron spin resonance-computed tomography/nitroxyl probe technique for non-invasive analysis of oxidative injuries. *Arch. Biochem. Biophys.* **2003**, *416*, 1–8.
- (5) Takeshita, K.; Ozawa, T. Recent progress in *in vivo* ESR spectroscopy. *J. Radiat. Res. (Tokyo)* **2004**, *45*, 373–384.
- (6) Soule, B. P.; Hyodo, F.; Matsumoto, K.; Simone, N. L.; Cook, J. A.; Krishna, M. C.; Mitchell, J. B. Therapeutic and clinical applications of nitroxide compounds. *Antioxid. Redox Signaling* **2007**, *9*, 1731–1743.
- (7) Afzal, V.; Brasch, R. C.; Nitecki, D. E.; Wolff, S. Nitroxyl spin label contrast enhancers for magnetic resonance imaging. Studies of acute toxicity and mutagenesis. *Invest. Radiol.* **1984**, *19*, 549–552.

- (8) Matsumoto, K.; Hyodo, F.; Matsumoto, A.; Koretsky, A. P.; Sowers, A. L.; Mitchell, J. B.; Krishna, M. C. High-resolution mapping of tumor redox status by MRI using nitroxides as redox-sensitive contrast agents. *Clin. Cancer Res.* **2006**, *12*, 2455–2462.
- (9) Hyodo, F.; Matsumoto, K.; Matsumoto, A.; Mitchell, J. B.; Krishna, M. C. Probing the intracellular redox status of tumors with MRI and redox-sensitive contrast agents. *Cancer Res.* **2006**, *66*, 9921–9928.
- (10) Hyodo, F.; Matsumoto, K.; Matsumoto, A.; Mitchell, J. B.; Krishna, M. C. Probing the intracellular redox status of tumors with MRI and redox-sensitive contrast agents. *Cancer Res.* **2006**, *66*, 9921–9928.
- (11) Hyodo, F.; Chuang, K.-H.; Goloshevsky, A. G.; Sulima, A.; Griffiths, G. L.; Mitchell, J. B.; Koretsky, A. P.; Krishna, M. C. Brain redox imaging using blood-brain barrier-permeable nitroxide MRI contrast agent. *J. Cereb. Blood Flow Metab.* **2008**, 1–10.
- (12) Myiake, M.; Shen, J.; Liu, S.; Shi, H.; Liu, W.; Yuan, Z.; Pritchard, A.; Kao, J. P. Y.; Liu, K. J.; Rosen, G. M. Acetoxymethoxycarbonyl nitroxides as EPR proimaging agents to measure O<sub>2</sub> levels in mouse brain: A pharmacokinetic and pharmacodynamic study. *J. Pharmacol. Exp. Ther.* **2006**, *318*, 1187–1193.
- (13) Shen, J.; Liu, S.; Miyake, M.; Liu, W.; Pritchard, A.; Kao, J. P. Y.; Rosen, G. M.; Tong, Y.; Liu, K. J. Use of 3-acetoxymethoxycarbonyl-2,2,5,5-tetramethyl-1-pyrrolidinyloxyl as an EPR oximetry probe: Potential for *in vivo* measurement of tissue oxygenation in mouse brain. *Magn. Reson. Med.* **2006**, *55*, 1433–1440.
- (14) Sano, H.; Naruse, M.; Matsumoto, K.; Oi, T.; Utsumi, H. A new nitroxyl-probe with high retention in the brain and its application for brain imaging. *Free Radical Biol. Med.* **2000**, *28*, 959–969.
- (15) Anzai, K.; Saito, K.; Takeshita, K.; Takahashi, S.; Miyazaki, H.; Shoji, H.; Lee, M. C.; Masumizu, T.; Ozawa, T. Assessment of ESR-CT imaging by comparison with autoradiography for the distribution of a blood-brain-barrier permeable spin probe, MC-PROXYL, to rodent brain. *Magn. Reson. Imaging* **2003**, *21*, 765–772.
- (16) Cotrim, A. P.; Hyodo, F.; Matsumoto, K.; Sowers, A. L.; Cook, J. A.; Baum, B. J.; Krishna, M. C.; Mitchell, J. B. Differential radiation protection of salivary glands versus tumor by tempol with accompanying tissue assessment of tempol by magnetic resonance imaging. *Clin. Cancer Res.* **2007**, *13*, 4928–4933.
- (17) Zhang, L.; Zhu, H.; Oprea, T. I.; Golbraikh, A.; Tropsha, A. QSAR modeling of the blood-brain barrier permeability for diverse organic compounds. *Pharm. Res.* **2008**, *25*, 1902–1914.
- (18) Shen, D. D.; Artru, A. A.; Adkison, K. K. Principles and applicability of CSF sampling for the assessment of CNS drug delivery and pharmacodynamics. *Adv. Drug Delivery Rev.* **2004**, *56*, 1825–1857.

membranes, etc.) often serve as a major approach for indirect evaluation of drug delivery in the brain tissue. The development of new methodologies for *in vivo* imaging of BBB permeability, which are noninvasive, environmentally friendly, with minimal animal loss and minimal risk for volunteers, is a major goal of the modern pharmaceutical industry.

Currently, the radiopharmaceuticals combined with autoradiography or positron-emission tomography (PET) are the only option for noninvasive real-time imaging of BBB permeability.<sup>23–25</sup> Despite that this approach is highly sensitive and valuable, it suffers from several restrictions to be widely applicable in preclinical and clinical testing of new therapeutics. The radiolabeling possesses a risk for human safety and requires special experimental equipment and facilities, which increases markedly the cost of this analysis. The radiotracers are usually used for labeling of diagnostic markers, but not for labeling of therapeutics and noninvasive imaging of their permeability and localization in different organs.

In the present study, we would like to introduce a novel nonradioactive and environmentally friendly alternative for noninvasive real-time imaging of BBB permeability for conventional drugs, using stable nitroxyl radicals as spin-labels and MRI. To clarify the advisability of this approach, we have to prove that (i) the nitroxyl-labeled drug is stable in physiological fluids and there is no dissociation of nitroxyl-drug bond in the blood; and (ii) the nitroxyl-labeling does not affect significantly the drug pharmacodynamics, its toxicity and permeability for BBB.

We considered the anticancer drug lomustine [1-(2-chloroethyl)-3-cyclohexyl-1-nitrosourea, CCNU] as an appropriate model for spin-labeling and nitroxyl radical TEMPO as an appropriate spin-label for this particular case. Lomustine has a significant impact in the improvement of the health-

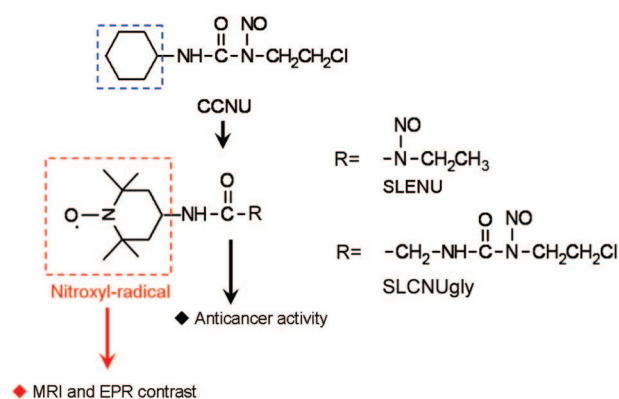


**Figure 1.** (A) Lomustine (CCNU) and its nitroxyl-labeled analogues (SLENU and SLCNUgly).

related quality of life of patients, treated for brain tumors, as well as of any other patients with cancer.<sup>26</sup> Both substances (TEMPO-radical and lomustine) are permeable for BBB,<sup>16,27</sup> and the TEMPO radical has a 6-membered ringed structure as the cyclohexyl part of lomustine molecule.

The lomustine molecule could be formally separated into two parts (Figure 1). The nitrosourea ensures the anticancer effect and could not be modified. Thus, the cyclohexyl part of lomustine was exchanged with TEMPO radical. We supposed that this substitution keeps a low risk for influence of drug pharmacodynamics in the organism, its toxicity and anticancer effect.

Two TEMPO-labeled analogues (SLENU and SLCNUgly) of lomustine (originally synthesized) (Figure 1) and one commercial nitroxyl (TEMPOL) were used in EPR and MRI experiments. All substances were characterized with different hydrophobicity [classified as slightly hydrophobic (TEMPOL), hydrophobic (SLENU), and strongly hydrophobic (SLCNUgly)], cell permeabilization ability and blood clearance. Thus, it was possible to investigate the relationship between the structure of nitroxyl-labeled drug, its half-life in the circulation, its permeability for BBB and MRI signal dynamic in the brain. This information was important for estimation of the merits and demerits of the described approach and finding pathways for overcoming the restrictions.

## Experimental Methods

**Chemicals.** TEMPOL (4-hydroxy-2,2,6,6-tetramethyl-1-piperidin-1-oxyl) was purchased from Sigma-Aldrich.

Nitroxyl-labeled nitrosoureas SLENU {1-ethyl-3-[4-(2,2,6,6-tetramethylpiperidine-1-oxyl)]-1-nitrosourea} and SLCNUgly {1-chloroethyl-3-[4-glycine-(2,2,6,6-tetramethyl-1-piperidin-1-oxyl)]-1-nitrosourea} were synthesized according to the method described by J. J. A. Frenay et al.<sup>28</sup>

- (19) Pan, D.; Iyer, M.; Liu, J.; Li, Y.; Hopfinger, A. J. Constructing optimum blood brain barrier QSAR models using a combination of 4D-molecular similarity measures and cluster analysis. *J. Chem. Inf. Comput. Sci.* **2004**, *44*, 2083–2098.
- (20) Dash, A. K.; Elmquist, W. F. Separation methods that are capable of revealing blood-brain barrier permeability. *J. Chromatogr., B: Anal. Technol. Biomed. Life Sci.* **2003**, *797*, 241–254.
- (21) Gumbleton, M.; Audus, K. L. Progress and limitations in the use of *in vitro* cell cultures to serve as a permeability screen for the blood-brain barrier. *J. Pharm. Sci.* **2001**, *90*, 1681–1698.
- (22) Killian, D. M.; Gharat, L.; Chikhale, P. J. Modulating blood-brain barrier interactions of amino acid-based anticancer agents. *Drug Delivery* **2000**, *7*, 21–25.
- (23) Josseland, V.; Pélerin, H.; de Bruin, B.; Jegou, B.; Kuhnast, B.; Hinnen, F.; Ducongé, F.; Boisgard, R.; Beuvon, F.; Chassoux, F.; Daumas-Duport, C.; Ezan, E.; Dollé, F.; Mabondzo, A.; Tavittian, B. Evaluation of drug penetration into the brain: a double study by *in vivo* imaging with positron emission tomography and using an *in vitro* model of the human blood-brain barrier. *J. Pharmacol. Exp. Ther.* **2006**, *316*, 79–86.
- (24) Abbott, N. J.; Chugani, D. C.; Zaharchuk, G.; Rosen, B. R.; Lo, E. H. Delivery of imaging agents into brain. *Adv. Drug Delivery Rev.* **1999**, *37*, 253–277.
- (25) Weissleder, R.; Mahmood, U. Molecular imaging. *Radiology* **2001**, *219*, 316–333.

- (26) Taphoorn, M. J. B.; Van den Bent, M. J.; Mauer, M. E. L.; Coens, C.; Delattre, J.-Y.; Brandes, A. A.; Smitt, P. A. E.; Besnens, H. J. J. A.; Frenay, M.; Tjissen, C. C.; Lacombe, D.; Allgeier, A.; Bottomley, A. Health-related quality of life in patients treated for anaplastic oligodendroma with adjuvant chemotherapy: Results of a European Organisation for Research and Treatment of Cancer Randomized Clinical Trial. *J. Clin. Oncol.* **2007**, *25*, 5723–5730.
- (27) Bodor, N.; Buchwald, P. Recent advances in the brain targeting of neuropharmaceuticals by chemical delivery systems. *Adv. Drug Delivery Rev.* **1999**, *36*, 229–254.



ylpiperidine-1-oxyl)]-1-nitrosoarea} were synthesized and purified according to Gadjeva et al.<sup>28,29</sup> (with slight modifications).

Deionized water (deionization by the Milli-Q system) was used for all experiments. Other chemicals used were of analytical or HPLC grade.

**In Vitro EPR measurements.** SLENU, SLCNUgly, and TEMPOL were first dissolved in DMSO to prepare 200 mM stock solutions. These 200 mM solutions were diluted with PBS, containing 1% bovine serum albumin to prepare 2 mM standard solutions. Each solution was put into a glass capillary, and their X-band EPR spectra were measured on X-band EPR instrument (JEOL, Akishima, Japan) with a TE-mode cavity. The capillary tube was positioned in the center of the TE-mode cavity using a special sample holder. The measurements were made under the following conditions: microwave frequency = 9.4 GHz, magnetic field strength = 336 mT, microwave power = 2.0 mW, field modulation frequency = 100 kHz, field modulation amplitude = 0.063 mT, time constant = 0.01 s, sweep width = 10 mT, scan time (sweep time) = 1 min.

In parallel, 2  $\mu$ L of 200 mM stock solutions of SLENU, SLCNUgly, or TEMPOL (in DMSO) were added to 198  $\mu$ L freshly isolated blood (with heparin) and the EPR measurements were provided at the parameters mentioned above within 30 min scan time.

The rotational correlation time ( $\tau_c$ ) of nitroxyl derivatives in PBS and blood was calculated by the following equation (Figure 2).<sup>30</sup>

$$\tau_c = A\{R(-1) + R(+1) - 2\} \cdot \Delta H(0) \quad (1)$$

$R(-1) = [I(0)/I(-1)]^{1/2}$ , where  $I(0)$  and  $I(-1)$  are the amplitudes of line 2 and line 3 in the EPR spectrum, respectively;  $R(+1) = [I(0)/I(+1)]^{1/2}$ , where  $I(0)$  and  $I(+1)$  are the amplitudes of line 2 and line 1 in the EPR spectrum, respectively;  $\Delta H(0)$  is a line 2 width;  $A = 6.6 \times 10^{-10}$  s is a constant, calculated for TEMPOL radical.

All calculations were made from the EPR spectra of the nitroxyl derivatives (2 mM) in PBS or freshly isolated blood from mouse (after 5 min incubation). In the text, the data are presented as mean values from three independent experiments (SD did not exceed 5%). The obtained values are approximated, since we used an A-value for TEMPOL in all calculations.

The total nitroxyl concentration in the brain tissue was analyzed according to Hyodo et al.<sup>10</sup> In brief, the brain was isolated 10 min after the iv injection of nitroxyl derivative in the mouse (0.4 mmol/kg bw). The isolated brain was

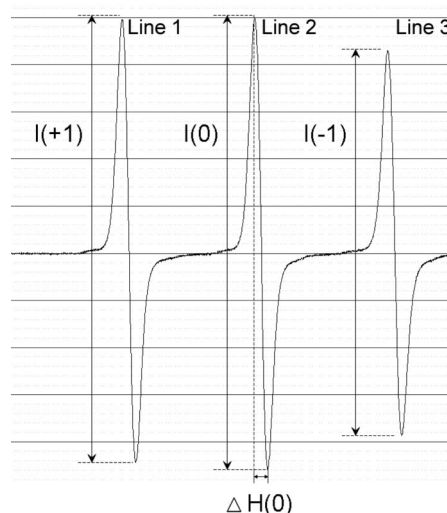


**Figure 2.** X-band EPR spectrum of TEMPOL radical in PBS (pH 7.4) and characteristics used in the calculation of the rotational correlation time ( $\tau_c$ ).

rinsed several times by cold PBS, and the tissue (in equal weight for each animal) was homogenized in cold PBS. Ferricyanide (200  $\mu$ L of 10 mM solution) was added to each homogenate (800  $\mu$ L) to convert the reduced nitroxyl derivatives to their oxidized forms. EPR signal intensity was measured in tissue homogenates under the following conditions: modulation frequency, 100 kHz; microwave power, 1 mW. Finally, the concentration of nitroxyl derivative in the brain tissue was calculated based on a dilution factor of 5.

**In Vivo EPR measurements.** The pharmacokinetic profiles of nitroxyl derivatives in mouse blood were measured using the method reported by Matsumoto et al.<sup>31</sup> C57Bl/6 mice (6 to 8 weeks of age at the time of experiments; mean weight ~25 g) were used. All experiments were conducted in accordance with the guidelines of the Physiological Society of Japan and were approved by the Animal Care and Use Committee of the National Institute of Radiological Sciences, Chiba, Japan.

The experimental design is shown in Scheme 2.

The mouse (~25 g) was anesthetized with 1.5% isoflurane using a face mask. The body temperature was kept within  $36 \pm 1$  °C. The tail and jugular veins were cannulated by polyethylene tubing (PE10, Intramedic, Becton Dickinson Co.). The PE10 tubing from the jugular vein was placed in the TE-mode cavity of EPR instrument (JEOL, Akishima, Japan). The end of the tubing was connected to the syringe. All tubing and syringes were heparinized. The nitroxyl derivative was injected intravenously through the tail vein (0.4 mmol/kg bw; the drugs were dissolved in DMSO), and immediately after the injection the blood (~100  $\mu$ L) was drained from the blood stream through the jugular vein to

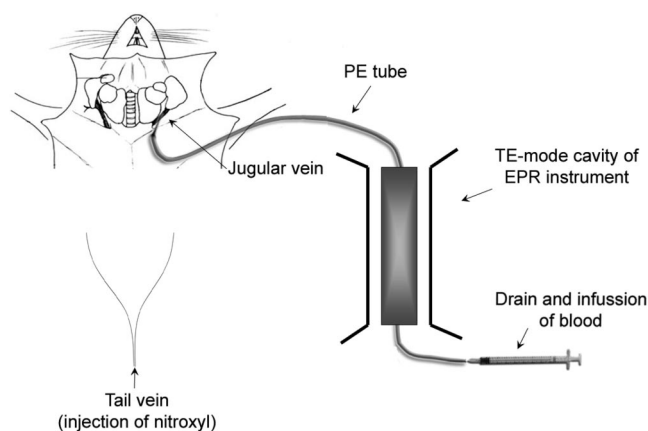
(28) Gadjeva, V. Structure-based design of nitrosoarenes containing tyrosine derivatives as potential antimelanoma agents. *Eur. J. Med. Chem.* **2002**, 37, 295–300.

(29) Zheleva, A.; Gadjeva, V. Spin labelled nitrosoarenes and triazenes and their non-labelled clinically used analogues—a comparative study on their physicochemical properties and antimelanomic effects. *Int. J. Pharmacol.* **2001**, 212, 257–266.

(30) Hayashi, H.; Iwasaki, T.; Onodera, Y.; Nagase, T.; Itabashi, O. *Tohoku Kogyo Gijutsu Shikenjo Houkoku* **1992**, 29, 33.

(31) Matsumoto, K.; Krishna, M. C.; Mitchell, J. B. Novel pharmacokinetic measurement using electron paramagnetic resonance spectroscopy and simulation of in vivo decay of various nitroxyl spin probes in mouse blood. *J. Pharmacol. Exp. Ther.* **2004**, 310, 1076–1083.

**Scheme 2.** Scheme of Imaging of EPR Signal Dynamic of Nitroxyl Radical in the Blood Stream of Mouse under Anesthesia



reach the TE-mode cavity of the EPR instrument. The EPR measurement was started. Immediately after finishing the measurement, the blood was infused back to the blood stream of the mouse. This cycle was repeated every 4–5 min within 30 min, to register the EPR signal dynamic of nitroxyl radical after its intravenous injection in the anesthetized animal. The EPR measurements were carried out in the same manner as described above.

**In Vivo MRI Measurements.** MRI measurements were performed on a 7.0 T horizontal magnet (Kobelco and Jastec, Japan) interfaced to a Bruker Avance console (Bruker BioSpin, Germany) and controlled with ParaVision 4.0.1 (Bruker BioSpin, Germany).

The mouse (C57Bl/6, ~25 g) was anesthetized by isoflurane (1.2%) and placed in a head holder (Rapid Biomedical, Germany), stomach-side down and fixed head. A respiration sensor (SA Instruments, NY) was placed on the back of the mouse. A nonmagnetic temperature probe (FOT-M and FTI-10, FISO Technology, Germany) was used to monitor the rectal temperature of the mouse. The tail vein was cannulated by polyethylene tubing (PE10, Becton-Dickinson, NJ, USA) for injection of drug. The mouse was then placed in the  $^1\text{H}$ -volume radiofrequency (RF) resonator (Bruker BioSpin) with surface RF receiver (Rapid Biomedical, Germany), which was previously warmed up using a body temperature controller (Rapid Biomedical). The resonator units, including the mouse, were placed in the magnet bore. The mouse body temperature was kept at  $37 \pm 1^\circ\text{C}$  during the MR measurements. Before the measurements after drug injection, five control images of the mouse brain were taken with the following parameters:  $T_1$ -weighted incoherent gradient-echo sequence (fast low-angle shot; FLASH), repetition time (TR) = 75 ms; echo time (TE) = 3.5 ms; flip angle (FA) = 45 degrees; field of view (FOV) =  $3.2 \times 3.2$  cm; number of averages = 4; scan time = 19.6 s; matrix =  $64 \times 64$ ; slice thickness = 1.0 mm; number of slices = 4. We selected coronal slice orientations with a  $500 \mu\text{m} \times 500 \mu\text{m} \times 1000 \mu\text{m}$  nominal voxel resolution. One minute and 40 s after starting the scan, 100  $\mu\text{L}$  of SLENU, SLCNUgly or TEMPOL (final dose, 0.4 mmol/kg bw; the

drugs were dissolved in DMSO) was injected via the tail vein.  $T_1$ -weighted images were acquired continuously within ~20 min.

Mice, injected with DMSO only (in the same volume, 100  $\mu\text{L}$ ) served as controls.

The MRI data were analyzed using the ImageJ (National Institutes of Health, MD, USA) software.

All experiments were conducted in accordance with the guidelines of the Physiological Society of Japan and were approved by the Animal Care and Use Committee of the National Institute of Radiological Sciences, Chiba, Japan.

## Results and Discussion

The substitution of the cyclohexyl part of the lomustine molecule with nitroxyl radical, as well as the substitution at the fourth position of the piperidine ring, did not affect significantly the toxicity and anticancer activity of nitrosoarea. Using wild-type C57Bl/6 mice, we established the following LD50 values for nitroxyl derivatives: ~210 mg/kg bw for TEMPOL, ~100 mg/kg bw for SLENU, and ~125 mg/kg bw for SLCNUgly, versus ~56 mg/kg bw for lomustine (CCNU). The nitroxyl radical in SLENU and SLCNUgly decreased the toxicity of nitrosoarea.

Using C57Bl/6 mice with experimental lymphoma L1210, we established the following optimal doses for anticancer activity of SLENU, SLCNUgly, and CCNU: ~45 mg/kg bw for SLENU and SLCNUgly, versus ~20 mg/kg for CCNU.

These preliminary data allowed the selection of the optimal dose for *in vivo* EPR and MR imaging of nitroxyl derivatives in C57Bl/6 mice. The doses, combining a comparatively low toxicity and comparatively high EPR and MRI contrast characteristics, were in the interval 0.2–0.4 mmol/kg bw, below the toxic limit or slightly close to the LD50 values of the described nitroxyl derivatives.

The first step of our study was to ensure that the TEMPO–nitrosoarea bond is stable and there is no dissociation between both compounds in the blood. Thus, the detection of MRI signal enhancement of nitroxyl radical *in vivo* will indicate the localization of nitrosoarea in the brain tissue.

In PBS, the normalized EPR spectra of TEMPOL, SLENU, and SLCNUgly were distinguished by the amplitude of the third line in the triplet [ $I(-1)$ ] (Figure 3A). The lower amplitudes of line 3 in the EPR spectrum of SLENU and SLCNUgly could be explained by the limited motion of the nitrosoarea-conjugated nitroxyl radical in comparison with free TEMPOL radical (in the TEMPOL molecule). The larger the substitute at the fourth position of the piperidine ring, the slower the motion of the nitroxyl radical, which results in lower EPR signal enhancement. In PBS, the rotational correlations times ( $\tau_c$ ) of nitroxyl derivatives were  $10.56 \times 10^{-12}$  s,  $29.45 \times 10^{-12}$  s, and  $31.38 \times 10^{-12}$  s for TEMPOL, SLENU, and SLCNUgly, respectively.

In blood, the normalized EPR spectra had the same profiles as in PBS. There were no changes in the shape of the EPR spectra of SLENU and SLCNUgly during long-term incuba-

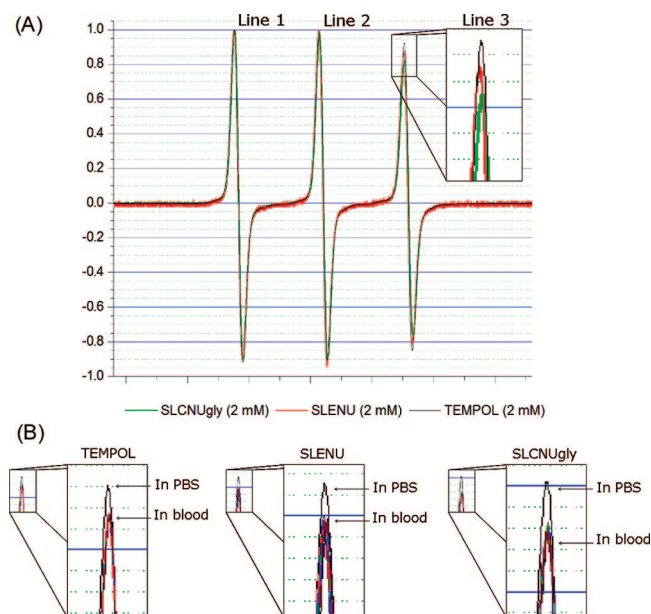


**Figure 3.** (A) Normalized EPR spectra of SLENU, SLCNUgly, and TEMPOL in PBS. In blood, the EPR spectra of all substances have same profiles. (B) Amplitudes of line 3 during long-term incubation of SLENU, SLCNUgly, and TEMPOL in freshly isolated blood samples *in vitro* (1–30 min). The amplitude of line 3 in PBS is shown for comparison.

tion in blood (Figure 3B), which indicated that there was no dissociation of the TEMPO–nitrosoarea covalent bond. Only the amplitude of line 3 decreased in blood in comparison with PBS (Figure 3B). The rotational correlations times ( $\tau_c$ ) of nitroxyl derivatives in blood were  $20.33 \times 10^{-12}$  s,  $32.87 \times 10^{-12}$  s, and  $46.20 \times 10^{-12}$  s for TEMPOL, SLENU, and SLCNUgly, respectively. The data suggest that the motion of nitroxyl radical in blood decreased for each derivative, regardless of its hydrophobicity, presumably as a result of interaction between the drug and blood cells and/or lipoproteins.

In the second step, we investigated the blood clearance of nitroxyl derivatives *in vivo* in mice, using EPR spectroscopy (Scheme 2). This information allowed a prediction of the time necessary for transportation of nitroxyl derivative in the brain tissue (if it crosses BBB), which was important for design of the MRI measurements.

The kinetic curves of EPR signal dynamics of nitroxyl derivatives in the blood stream of living mice are shown in Figure 4. They were characterized with two phases: (i) an increase of the EPR signal within 1–1.5 min after the drug injection; and (ii) a decrease of the EPR signal within 1–5 min after the drug injection. The first phase is mainly a result of initial enhancement of the drug concentration in the blood stream. The second phase is probably a result of the following processes: (i) a reduction of nitroxyl radical in the blood plasma; and/or (ii) transportation of the drug from the blood stream to the blood cells and/or tissues and further reduction of nitroxyl radical from the cell/tissue reducing equivalents.

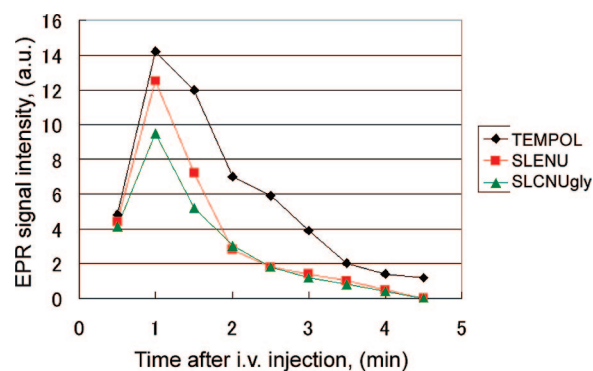


**Figure 4.** Dynamics of the EPR signal in the blood stream of mice under anesthesia after intravenous (iv) injection of nitroxyl derivative (0.4 mmol/kg bw). Mean values from three independent experiments are presented in the figure (SD values did not exceed 30%).

The time-decay of the EPR signal *in vivo* correlated with the hydrophobicity of nitroxyl derivative and its cell permeability. The rate of time-decay was slower for the low hydrophobic TEMPOL and faster for the hydrophobic SLENU and strongly hydrophobic SLCNUgly.

*In vivo*, the EPR signal of all nitroxyl derivatives disappeared rapidly in the blood (within 4–5 min after their injection). However, *in vitro* (in isolated blood samples), their EPR signal was comparatively stable within 1–30 min incubation (only ~5% decrease was detected within this time interval). Since all investigated nitroxyls were cell permeable, we may speculate that within 4–5 min the nitroxyl derivatives were delivered in the tissues.

In the third step of our study, the nitroxyl derivatives were injected intravenously in healthy mice via the tail vein and  $^1\text{H}$ -MR imaging of the brain was performed on a 7.0 T horizontal MRI (Figure 5). The injected dose was 0.4 mmol/kg bw.

At the selected scanning parameters, the nitroxyl-radical manifested a good  $T_1$  relaxivity and was detected in the brain (Figure 5). Other authors<sup>8,9</sup> have also demonstrated a good  $T_1$  relaxivity of TEMPOL at similar concentrations on experimental phantoms and animals (mice) using 4.7 T MRI and high image resolution ( $128 \times 128$  or  $256 \times 256$ ). Although nitroxyls have a lower relaxivity than conventional  $T_1$  contrast agents such as gadolinium complexes, the volume distribution of nitroxyls is sufficiently greater because of better cell permeability,<sup>35</sup> and with improved sensitivity of

- (32) Matsumoto, K.; Yakumaru, H.; Narazaki, M.; Nakagawa, H.; Anzai, K.; Ikehira, H.; Ikota, N. Modification of nitroxyl contrast agents with multiple spins and their proton  $T_1$  relaxivity. *Magn. Reson. Imaging* **2008**, *26*, 117–121.
- (33) Metz, J. M.; Smith, D.; Mick, R.; Lustig, R.; Mitchell, J.; Cherakuri, M.; Glatstein, E.; Hahn, S. M. A phase I study of topical Tempol for the prevention of alopecia induced by whole brain radiotherapy. *Clin. Cancer Res.* **2004**, *10*, 6411–6417.
- (34) Ravizza, R.; Cereda, E.; Monti, E.; Gariboldi, M. B. The piperidine nitroxide Tempol potentiates the cytotoxic effects of Temozolomide in human glioblastoma cells. *Int. J. Oncol.* **2004**, *25*, 1817–1822.



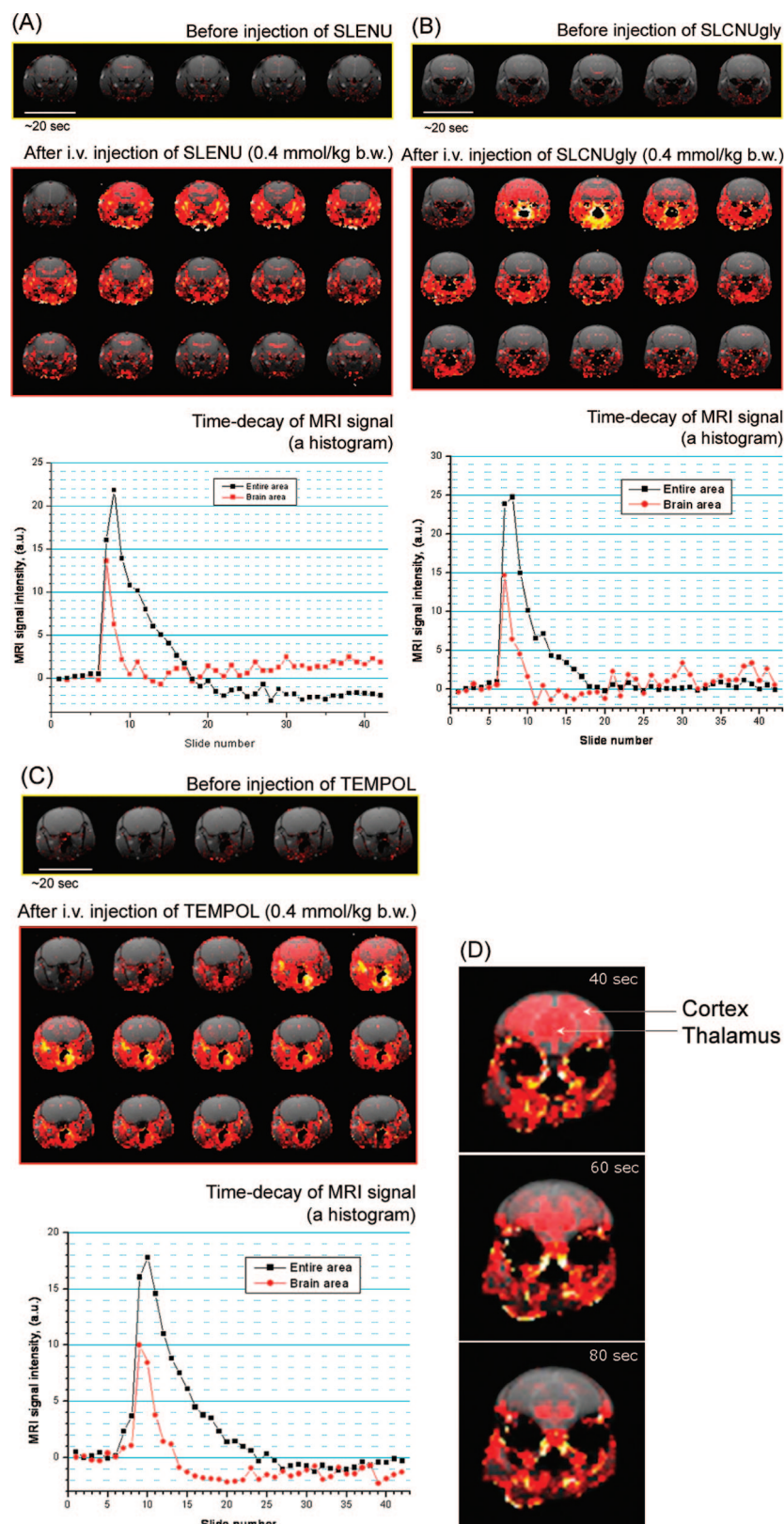


**Figure 5.** MRI signal dynamics of SLENU (A), SLCNUgly (B), and TEMPOL (C) in the brain and surrounding tissues after iv injection in mice (0.4 mmol/kg bw). Each image was obtained within a 20 s interval using a gradient-echo  $T_1$ -weighted MRI. The red color in the images is the extraction of the signal between every single slide and the averaged baseline signal (first 5 slides: before injection). The red and black colors in the chart represent MRI signal dynamics in the brain or entire area, respectively. A representative image from three independent experiments is shown in the figure. (D) MRI signal dynamics of SLENU in the brain compartments (cortex and thalamus) after its iv injection in mice (0.8 mmol/kg bw).

MRI and shift to higher magnetic fields, it is possible to detect nitroxyl radical in the tissues at low (nontoxic or low toxic) concentrations. In our study, using 7 T MRI and resolution  $64 \times 64$ , the MRI contrast of TEMPOL was high enough to detect the signal in the brain at concentrations 0.4 mmol/kg bw.

It is well-known that the nitrosoureas are highly permeable for cell membranes and BBB and are concentrated in the brain tissue. Therefore, it could be expected that the real concentration of SLENU and SLCNUgly in the brain tissue would be same as or even higher than the concentration of TEMPOL, and this should have a positive effect on MRI contrast of both nitroxyl-labeled drugs. We established that  $\sim 30\%$  of the injected dose of SLENU and SLCNUgly was localized in the brain. The experiments were performed on tissue homogenates prepared from perfused brain, isolated 10 min after the iv injection of the drug.

The MRI-signal dynamics of SLENU and SLCNUgly (Figure 5A,B) in the brain and surrounding tissues followed almost the same kinetics and distribution as nonconjugated TEMPO radical (Figure 5C). The maximum change in the signal intensity ( $\sim 25\text{--}30\%$  in comparison with the preinjection image) in the brain tissue was detected 20, 20 or 80 s after the injection of SLENU, SLCNUgly, or TEMPOL, respectively. In the brain tissue, the MRI signal intensity decreased during the subsequent 2 min, while in the surrounding tissues, the MRI signal intensity decreased during the subsequent 4–5 min. Recently, Hyodo et al. have reported that the MRI signal of a BBB permeable nitroxyl, methoxycarbonyl-2,2,5,5-tetramethylpyrrolidine-1-oxyl, also disappeared quickly after its transportation from the blood vessels to the brain tissue, despite the slower reduction rate of pyrrolidine radical.<sup>11</sup>

SLENU and SLCNUgly were rapidly and randomly distributed into the brain tissue. For example, the nitroxyl derivatives were localized predominantly in the cortex and thalamus (Figure 5D). The MRI signal decay in the cortex was faster than the MRI signal decay in the thalamus. It may be speculated that the cortex has a higher reduction potential than the thalamus. Similar results were reported by Hyodo et al.<sup>11</sup>

Obviously, the exchange of the cyclohexyl part of lomustine with TEMPO radical did not suppress the permeability of the drug for the BBB. All investigated nitroxyl derivatives (TEMPOL, SLENU, SLCNUgly) manifested a similar permeability. This assumption was confirmed by using EPR spectroscopy for the assessment of the total concentration of nitroxyl derivative (converted to its oxidized form) in the brain tissue, isolated 10 min after the drug injection into mice. It was observed that the normalized EPR signal intensity of tissue homogenates, isolated from SLENU- and SLCNUgly-treated mice ( $2.3 \pm 0.6$  and  $2.5 \pm 0.4$  a.u. per g of tissue, respectively), was slightly higher than the EPR signal

intensity of homogenates, isolated from TEMPOL-treated mice ( $2.0 \pm 0.5$  a.u. per g of tissue). The data from diffusion-weighted MRI also confirmed that SLENU and SLCNUgly crossed the BBB. After free-water signal suppression by the diffusion-weighted MRI technique with motion probing gradients, the MRI signal remained in the brain tissue (data are not shown).

The MRI signal enhancement of nitroxyl radical disappeared quickly (within 2–3 min) after the transportation of SLENU and SLCNUgly from the brain vessels in the brain tissue. Presumably, this is due to the high permeability of nitroxyl-labeled nitrosoureas for cell membranes, which is accompanied with rapid reduction of nitroxyl radical to the respective hydroxylamine in the brain cells and loss of MRI signal enhancement. In the surrounding tissues, the MRI signal was more stable, with a bit longer half-life.

There was a good correlation between the rate of blood clearance of nitroxyl derivatives and their MRI signal dynamic in the brain and surrounding tissues. The faster the blood clearance of the drug (SLCNUgly = SLENU > TEMPOL), the faster the appearance of the MRI signal of the nitroxyl derivative in the brain and surrounding tissues (SLCNUgly = SLENU > TEMPOL) (Figures 4, 5).

The fast detection of MRI signal enhancement could be considered as an advantage, because of shortening of the time of analytical and diagnostic process.

The present data are just a first trial for using nitroxyl radicals for spin-labeling of conventional drugs and noninvasive dynamic MR imaging of their permeability for the BBB. We tried to show the advisability of this concept. Novel synthetic strategies are necessary to increase the contrast of nitroxyl label and to improve its stability in the brain tissue without affecting the drug permeability for BBB. This will allow a higher spatial resolution of signal-to-noise ratio and will facilitate the real-time MRI data reconstruction and quantitative analysis.

The enhancement of the MRI contrast of nitroxyl label is important for the wide application of the described methodology. This is a limiting factor, currently requiring the application of nitroxyl-labeled drug in a comparatively high concentration (0.2–0.4 mmol/kg bw), which sometimes could be near or over the toxic limit.

There are two promising strategies to increase the MRI contrast of nitroxyl label in the brain and other tissues: (i) the exchange of six-membered ringed nitroxyl TEMPOL with five-membered ringed nitroxyl (2,2,5,5-tetramethylpyrrolidinyl-1-oxyl, PROXYL), which is characterized by higher relaxivity and  $\sim 10$  times higher resistance to bioreduction than TEMPOL radical;<sup>2</sup> and (ii) to develop new nitroxyl probes by modification of nitroxyl contrast agents with multiple spins (2 or more nitroxyl radicals bound covalently).

Matsumoto and colleagues have reported that a probe, consisting of three covalently bound PROXYL radicals, is characterized with 4-fold higher  $T_1$  relaxivity than a single PROXYL radical. However, it is still unclear whether these multinitroxyl probes are permeable for BBB, cells and other tissues, to be applicable for labeling of conventional drugs

(35) Hahn, S. M.; Wilson, L.; Krishna, C. M.; Liebmann, J.; DeGraff, W.; Gamson, J.; Amuni, A.; Venzon, S.; Mitchell, J. Identification of nitroxide radioprotectors. *Radiat. Res.* **1992**, *123*, 87–93.



and noninvasive imaging of their localization in the organism. The low-molecular-weight cell- and BBB-permeable methoxycarbonyl-PROXYL seems promising for drug labeling and MR imaging in the brain. Recently, Hyodo and colleagues have used this nitroxyl derivative for evaluation of brain redox status by MRI. The MRI signal of methoxycarbonyl-PROXYL in the brain is comparatively high and stable within 4 min after the drug injection in mice. Our preliminary data also demonstrated that PROXYL is characterized with higher MRI contrast and slower MRI signal decay in the tissues (Figure 1S, Supporting Information). Currently, we are under way to clarify the applicability of PROXYL in the described methodology.

It is necessary also to note that nitroxyl radicals are low toxic and comparatively harmless for living organisms. One of the most famous commercially available nitroxyls, TEMPOL (hydroxyl-TEMPO), is in phase I of clinical trials, as a preventer of alopecia in radiation-treated cancer patients.<sup>32</sup> The combined application of nitroxyls and conventional chemotherapeutics increases the anticancer effect and sup-

presses the multidrug resistance.<sup>33</sup> Therefore, the nitroxyl-labeling could be considered as environmentally friendly and with minimal risk for humans. There is one more advantage in nitroxyl-labeling and imaging. The dynamic of MRI signal enhancement gives additional information for oxidation/reduction status of the brain tissue. This information could be useful for planning of conventional chemo- and radiotherapy of cancer and other diseases in the brain or other organs.

**Acknowledgment.** The technical support of Dr. Antoaneta Zheleva (Trakia University, Stara Zagora, Bulgaria) and Ms. Sayaka Shibata (Molecular Imaging Center, NIRS-Chiba, Japan) is gratefully acknowledged.

**Supporting Information Available:** Figure depicting the MRI signal dynamics of carbamoyl-PROXYL in the brain after iv injection in mice. This material is available free of charge via the Internet at <http://pubs.acs.org>.

MP800175K